# COLLISIONLESS PLASMA PRESHEATH IN A NON-UNIFORM MAGNETIC FIELD

H.H. Abou-gabal
Nuclear Engineering Department, Faculty of Engineering,
Alexandria University, Alexandria, Egypt

ABSTRACT

The plasma equation for the flow of a collisionless plasma with a finite-temperature particle source along a non-uniform magnetic field to a boundary is formulated. The dependence of the electrostatic potential profile on the magnetic field strength profiles, on the spatial distribution of the particle source and on the ions type is investigated. Different magnetic field profiles even with the same mirror ratio at the sheath edge give rise to different potential profiles. In the case of a non-uniform magnetic field, the particle source profile has a considerable effect on the potential. The energy gained by the ion when crossing the sheath increases as the ion mass increases.

*Keywords: Collisionless plasma, Magnetic field profile, Plasma sheath.*

*Nomenclature*

| | |
|---|---|
| $\langle\sigma v\rangle$ | ionization rate coefficient |
| $B_o$ | magnetic field strength at x = 0 |
| e | electron charge |
| K | Boltzmann constant |
| m | electron mass |
| M | ion mass |
| $n_n$ | neutral atom density |
| $n_o$ | electron density at the midpoint |
| q | ion charge |
| $T_e$ | electron temperature |
| $T_i$ | ion temperature |
| $v_\perp$ | perpendicular component of the ion velocity |
| $v_{//}$ | parallel component of the ion velocity |

## 1. INTRODUCTION

The problem of plasma flowing along a non-uniform magnetic field to a boundary is important for the research on fusion in magnetically confined plasmas as well as on plasma-aided manufacturing processes. The electrostatic potential, developed in the plasma when it comes in contact with a surface, plays an important role in the interaction of the plasma with the divertor or limiter plates in tokamaks or stellarators [1,2]. In the electron cyclotron resonance (ECR) etching apparatus, a divergent magnetic field is used to extract plasma from the microwave chamber and to confine it near the specimen [3].

The problem of plasma flow to a wall and the formation of a sheath has drawn attention since the first analysis was done by Tonks and Langmuir in the context of discharge plasmas [4]. Harrison and Thompson [5] treated this problem by solving analytically the plasma-sheath equation in plane geometry, assuming a collisionless plasma with a cold-ion source. Emmert *et al.* [6] improved the solution of the plasma-sheath equation by considering a finite-temperature ion source. Bissel and Johnson [7] solved the plasma equation considering a Maxwellian particle source, which differs from the source chosen by Emmert *et al.* They indicated that the form of the particle source has an influence on the results. However, these analyses are restricted to cases of unmagnetized plasmas or plasmas in a uniform magnetic field. Sato *et al.* [8] formulated the plasma- sheath equation for a collisionless plasma in a magnetic field that expands to walls with a monotonically decreasing axial profile. They adopted the same expression used by Emmert *et al.* for the ion source function and assumed Boltzmann electrons. In order to obtain an analytic solution, they introduced some simplifying approximations, which restrict the

analysis to small mirror ratios. Their results are obtained for a mirror ratio at the sheath edge less than 2. In practice, one often needs to consider magnetic field profiles with higher mirror ratios.

In this paper, an approach similar to the technique used by Sato *et al.* is followed to formulate the plasma equation in a nonuniform open magnetic field. However, all the integrals involved in the calculations of the plasma density, of the particle and energy fluxes to the sheath are performed numerically. This method does not require any simplifications and is capable to meet the practical needs for a solution to the plasma flow problem in a magnetic field with moderate to high magnetic mirror ratio. Moreover, the dependence of the potential profile on the magnetic field profile, on the spatial distribution of the particle source and on the ions type is investigated.

Section 2 contains the formulation of the integral form of the plasma equation in a nonuniform open magnetic field. In Section 3, the method of solution is presented while the results are presented and discussed in section 4. The conclusions are given in section 5.

## 2. PLASMA EQUATION

In this paper, we consider the collisionless plasma flow to a solid wall in the presence of axisymmetric magnetic field that is also symmetric about x=0 and decreases monotonically for x>0 as shown in Figure (1). The walls at x= $\pm$ L are assumed to be perfectly absorbing and electrically floating. The potential $\Phi(x)$ in the steady state is expected to drop monotonically in the axial direction for x>0 and the value at x=0 is defined as zero.

The ion's constants of motion are the energy

$$E = \frac{1}{2}M(v_\perp^2+v_\parallel^2)+q\,\Phi(x), \qquad (1)$$

and the magnetic moment

$$\mu = \frac{1}{2}Mv_\perp^2/B(x), \qquad (2)$$

where B(x) is the magnetic field strength at the point x.

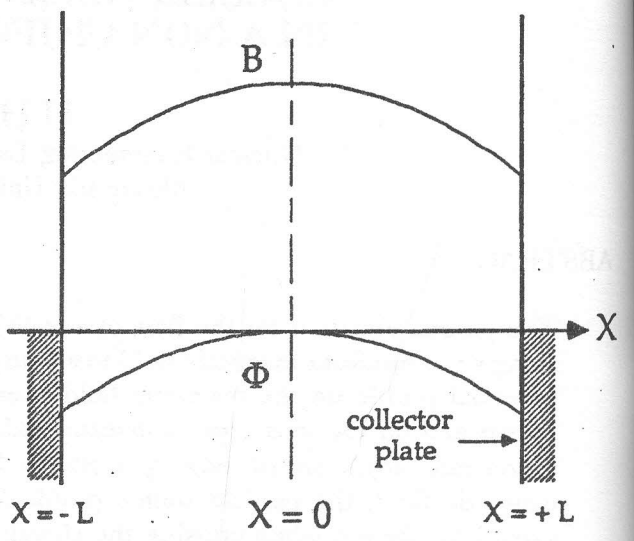


Figure 1. The geometry of the model and axial profiles of the potential and of the magnetic field strength.

Considering the plasma near the axis, neglecting radial dependence and integrating out the gyromotion, the kinetic equation in the phase space $(x,E,\mu)$ is described by

$$\sigma v''(x,E,\mu)\frac{\partial f(x,E,\mu,\sigma)}{\partial x} = S(x,E,\mu), \qquad (3)$$

where

$$v''(x,E,\mu) = \{2[E-\mu B(x)-q\,\Phi(x)]/M\}^{1/2}, \qquad (4)$$

$\sigma = +1$ denotes an ion moving to the right while $\sigma=-1$ denotes an ion moving to the left, $f(x,E,\mu,\sigma)$ is the ion distribution function and $S(x,E,\mu)$ is the distribution function of the ion source. Symmetry is assumed about x=0 in the sense that $S(x,E,\mu)=S(x,E,\mu)$ and $\Phi(x,E,\mu) = \Phi(-x,E,\mu)$. The boundary conditions for Eq. (3) are $f(-L,E,\mu,+1)=0$ and $f(L,E,\mu,-1)=0$.

The monotonically decreasing effective potential $\mu B(x)+q\Phi(x)$ causes all the originating ions to be accelerated towards the walls. The E-$\mu$ space can be separated into two regions, the reflected region and the passing region [8]. In the region such that $E<\mu B_o$, any originating ion cannot reach the center of the plasma, instead it is reflected at the turning point, $x_t(E,\mu)$, when $\sigma=-1$ and x>0 or when $\sigma=+1$ and x<0. $x_t(E,\mu)$ can be determined from

$$E - \mu B(x_t) - q\Phi(x_t)=0. \qquad (5)$$

In the region such that $E>\mu B_o$, all the originating ions pass through the plasma along the field lines without a change in direction of the motion. The distribution function $f(x,E,\mu,\sigma)$ can be obtained by integrating Eq. (3) using the appropriate boundary conditions. The sum of $f(x,E,\mu,+1)$ and $f(x,E,\mu,-1)$ in each region of the E-$\mu$ space can be written as [8]

$$\sum_{\sigma} f(x,E,\mu,\sigma)=\begin{cases} 2\int_0^L dx' \dfrac{S(x',E,\mu)}{v_{\parallel}(x',E,\mu)}, & E > \mu B_o, \\ 2\int_{x_t(E,\mu)}^L dx' \dfrac{S(x',E,\mu)}{v_{\parallel}(x',E,\mu)}, & E < \mu B_o, \end{cases} \qquad (6)$$

where x' is the point at which ions originate.

Using the normalizations

$\epsilon=E/KT_e$, $\Psi=-e\Phi/KT_e$, $\tau=T_e/T_i$, $s = x/L$,

$Z=q/e$, $R=B_o/B$, $V_{\perp} = v_{\perp}/v_{th}$, $V_{\parallel} = v_{\parallel}/v_{th}$,

where $v_{th}=\sqrt{\dfrac{2KT_i}{M}}$ and defining $\mu'=\mu B_o/KT_i$, Eq. (1) can be written as $\epsilon=\dfrac{V_{\perp}^2}{\tau}+\dfrac{V_{\parallel}^2}{\tau}-Z\psi(s)$. Similarly, we can write Eqs. (4)-(6) as following

$$V''(s,\epsilon,\mu')=[\tau\epsilon - \mu'/R(s) + Z\tau\psi(s)]^{1/2},$$

$$\tau\epsilon - \mu'/R(s_t) + Z\tau\psi(s_t) = 0,$$

where $s_t=x_t/L$ and

$$\sum_{\sigma} f(s,\epsilon,\mu',\sigma)=\begin{cases} 2\dfrac{L}{v_{th}}\int_0^1 ds' \dfrac{S(s',\epsilon,\mu')}{V_{\parallel}(s',\epsilon,\mu')} & \tau\epsilon>\mu', \\ 2\dfrac{L}{v_{th}}\int_{s_t(\epsilon,\mu')}^1 ds' \dfrac{S(s',\epsilon,\mu')}{V_{\parallel}(s',\epsilon,\mu')} & \tau\epsilon<\mu'. \end{cases} \qquad (7)$$

The ion density $n_i(x)$ is obtained by integrating $f(x,E,\mu,\sigma)$ over the E-$\mu$ space. Normalizing the ion density to $n_o$ and making use of the above normalizations and the Jacobians,

$$\partial(v_{\perp}^2,v_{\parallel})/\partial(V_{\perp}^2,V_{\parallel})=v_{th}^3 \text{ and } \partial(V_{\perp}^2,V_{\parallel})/\partial(\epsilon,\mu')=\tau/2V_{\parallel}R(s),$$

the normalized ion density, $N_i(s)$ can be determined from

$$N_i(s)=\frac{\pi v_{th}^3\tau}{2n_o R(s)}\sum_{\sigma}\int d\epsilon\int d\mu' \frac{f(s,\epsilon,\mu',\sigma)}{V_{\parallel}(s,\epsilon,\mu')}. \qquad (8)$$

Substituting Eq. (7) into Eq. (8), we obtain

$$N_i(s)= \frac{\pi v_{th}^2\tau L}{n_o R(s)}\left\{\int_0^{\infty}d\epsilon\int_0^{\tau\epsilon}d\mu'\frac{1}{V_{\parallel}(s,\epsilon,\mu')}\int_0^1 ds'\frac{S(s',\epsilon,\mu')}{V_{\parallel}(s',\epsilon,\mu')}\right.$$
$$+\int_{-Z\psi(s)}^0 d\epsilon\int_0^{\tau R(s)[\epsilon+Z\psi(s)]}d\mu'\frac{1}{V_{\parallel}(s,\epsilon,\mu')}\int_{s_t(\epsilon,\mu')}^1 ds'\frac{S(s',\epsilon,\mu')}{V_{\parallel}(s',\epsilon,\mu')}$$
$$\left.+\int_0^{\infty}d\epsilon\int_{\tau\epsilon}^{\tau R(s)[\epsilon+Z\psi(s)]}d\mu'\frac{1}{V_{\parallel}(s,\epsilon,\mu')}\int_{s_t(\epsilon,\mu')}^1 ds'\frac{S(s',\epsilon,\mu')}{V_{\parallel}(s',\epsilon,\mu')}\right\}. \qquad (9)$$

The electrons are electrostatically confined due to the presence of the sheath. This ensures enough collisionality to randomize their motion and hence their distribution function can be described by a Maxwell-Boltzmann distribution. For this distribution, the electron density at a point x is given by

$$n_e(x)=n_o\exp(e\Phi(x)/KT_e),$$

when normalized, it becomes

$$N_e(s)=n_e(x)/n_o=\exp(-\psi(s)). \qquad (10)$$

Considering that the plasma dimension is large compared with the Debye length, we can use the quasineutrality approximation to get $ZN_i = N_e$, which is called the plasma equation.

## 3. SOLUTION OF THE PLASMA EQUATION

To calculate the ion density, we use the same expression for the ion source chosen by Emmert *et al.* [6], namely

$$S(x,E,\mu) = \langle\sigma v\rangle n_o n_n h(x) \frac{M^2}{4\pi (KT_i)^2} v_{\parallel}(x,E,\mu) \exp\left(\frac{-[E - q\Phi(x)]}{KT_i}\right), \tag{11}$$

where h(x) expresses the spatial variation of the ionization rate.

Normalizing Eq. (11) and substituting it into Eq. (9), we obtain

$$\begin{aligned} N_i(s) = \frac{A\tau}{R(s)} \Bigg\{ & \int_0^{\infty} d\epsilon \int_0^{\tau\epsilon} d\mu' \frac{1}{V_{\parallel}(s,\epsilon,\mu')} \int_0^1 ds' h(s') e^{-\tau[\epsilon + Z\psi(s')]} \\ & + \int_{-Z\psi(s)}^{0} d\epsilon \int_0^{\tau R(s)[\epsilon + Z\psi(s)]} d\mu' \frac{1}{V_{\parallel}(s,\epsilon,\mu')} \int_{s_1(\epsilon,\mu')}^1 ds' h(s') e^{-\tau[\epsilon + Z\psi(s')]} \\ & + \int_0^{\infty} d\epsilon \int_{\tau\epsilon}^{\tau R(s)[\epsilon + Z\psi(s)]} d\mu' \frac{1}{V_{\parallel}(s,\epsilon,\mu')} \int_{s_1(\epsilon,\mu')}^1 ds' h(s') e^{-\tau[\epsilon + Z\psi(s')]} \Bigg\}, \end{aligned} \tag{12}$$

where $A = \langle\sigma v\rangle n_n L / v_{th}$.

In this work, an iteration method is used to solve for the normalized ion density distribution and the potential distribution function. An initial guess for the potential profile, $\Psi(s)$, is assumed. Integrations in Eq. (12) are performed numerically using both Trapezoid and Gauss Quadrature methods [9] to obtain the ion density distribution. The plasma equation is used to get a new potential profile which is resubstituted in Eq. (12) and so on until convergence is reached, namely when

$$\left| \frac{\psi_{new} - \psi_{old}}{\psi_{old}} \right| < \varepsilon,$$

for the whole region. $\varepsilon$ is a convergence criterion parameter.

In general, the ion source in the sheath can be neglected because of a small thickness of the sheath and a remarkable decrease in the ionization rate which is dependent on the electron density. Therefore, the requirement that the electron current and the ion current must be equal at the wall enables us to determine the wall potential, $\Psi_w$. The ion current, $\Gamma_i$, can be evaluated by the following integration

$$\Gamma_i(x) = 2\pi \sum_{\sigma} \int v_{\perp} dv_{\perp} \int dv_{\parallel} v_{\parallel} f(x, v_{\perp}, v_{\parallel}, \sigma). \tag{13}$$

The electron current, $\Gamma_e$, can be expressed as [8]

$$\Gamma_e = \left(\frac{KT_e}{2\pi m}\right)^{1/2} n_o \, e^{-\psi_w}. \tag{14}$$

Equating Eqs. (13) and (14) and performing the necessary normalizations with the use of the appropriate Jacobians, the wall potential, $\Psi_w$, can be obtained from

$$\begin{aligned} \psi_w = -\ln \Bigg[ \sqrt{\frac{4\pi m}{M\tau}} \frac{A\tau}{R_1} \Bigg\{ & \int_0^{\infty} d\epsilon \int_0^{\tau\epsilon} d\mu' \int_0^1 ds' h(s') e^{-\tau[\epsilon + Z\psi(s')]} \\ & + \int_{-Z\psi_1}^{0} d\epsilon \int_0^{\tau R_1[\epsilon + Z\psi_1]} d\mu' \int_{s_1(\epsilon,\mu')}^1 ds' h(s') e^{-\tau[\epsilon + Z\psi(s')]} \\ & + \int_0^{\infty} d\epsilon \int_{\tau\epsilon}^{\tau R_1[\epsilon + Z\psi_1]} d\mu' \int_{s_1(\epsilon,\mu')}^1 ds' h(s') e^{-\tau[\epsilon + Z\psi(s')]} \Bigg\} \Bigg], \end{aligned} \tag{15}$$

where $\Psi(s)$ is the converged solution for the normalized potential profile obtained as described above, $R_1 = R(1)$ and $\Psi_1 = \Psi(1)$ are the mirror ratio and the normalized potential respectively at the plasma-sheath boundary.

Similarly, the equality of these two equations allows us to obtain the mean velocity of the ions at the boundary, $\langle v_{\parallel} \rangle_1$, as

$$\langle v_{\parallel} \rangle_1 = Z \sqrt{\frac{KT_e}{2\pi m}} \, e^{\psi_1 - \psi_w}. \tag{16}$$

From Eq. (13), we can also obtain the normalized particle flux at the boundary as

$$\Gamma_1=\frac{\Gamma_i(1)}{n_o C_s}=\sqrt{\frac{2}{1+\tau}}A\tau\left\{\int_0^{\infty}d\epsilon\int_0^{\tau\epsilon}d\mu'\int_0^1 ds' h(s')e^{-\tau[\epsilon+Z\psi(s')]}\right.$$
$$+\int_{-Z\psi_1}^{0}d\epsilon\int_0^{\tau R_1[\epsilon+Z\psi_1]}d\mu'\int_{s_f(\epsilon,\mu')}^1 ds' h(s')e^{-\tau[\epsilon+Z\psi(s')]} \quad (17)$$
$$\left.+\int_0^{\infty}d\epsilon\int_{\tau\epsilon}^{\tau R_1[\epsilon+Z\psi_1]}d\mu'\int_{s_f(\epsilon,\mu')}^1 ds' h(s')e^{-\tau[\epsilon+Z\psi(s')]}\right\},$$

where $C_s=[K(T_e+T_i)/M]^{1/2}$ is the isothermal sound speed.

The normalized energy flux of the ions entering the sheath, $Q_1 = Q_i(1)/[n_o(KT_e+KT_i)C_s]$, can be calculated by integrating the product $(M/2)fv^2v_{//}$ over the phase space. After performing the necessary normalizations and variables transformations, we obtain

$$Q_1=\frac{\sqrt{2}}{(1+\tau)^{3/2}}A\tau\left\{\int_0^{\infty}d\epsilon\int_0^{\tau\epsilon}d\mu' V^2(1,\epsilon,\mu')\int_0^1 ds' h(s')e^{-\tau[\epsilon+Z\psi(s')]}\right.$$
$$+\int_{-Z\psi_1}^{0}d\epsilon\int_0^{\tau R_1[\epsilon+Z\psi_1]}d\mu' V^2(1,\epsilon,\mu')\int_{s_f(\epsilon,\mu')}^1 ds' h(s')e^{-\tau[\epsilon+Z\psi(s')]} \quad (18)$$
$$\left.+\int_0^{\infty}d\epsilon\int_{\tau\epsilon}^{\tau R_1[\epsilon+Z\psi_1]}d\mu' V^2(1,\epsilon,\mu')\int_{s_f(\epsilon,\mu')}^1 ds' h(s')e^{-\tau[\epsilon+Z\psi(s')]}\right\},$$

where $V^2=V_{\perp}^2+V_{//}^2$ at the plasma-sheath boundary. The integrations in Eqs. (15), (17) and (18) are solved numerically using both Trapezoid and Gauss Quadrature methods [9].

## 4. RESULTS AND DISCUSSION

A hydrogen plasma with equal ion and electron temperatures, i.e. $\tau=1$, is considered. Considering the fact that the ionization rate depends on the electron density, the expression for h(s) presented by Harrison and Thompson [5] is adopted here, namely,

$$h(s) = \exp(-\nu\,\psi(s)),$$

which allows the ion source to be proportional to the $\nu$ power of the electron density. In the following calculations $\nu$ is set equal to 1. The magnetic field mirror ratio profile R(s) is assumed to be expressed in the same form used by Sato *et al.* [8] and which is written as

$$R(s) = \exp(\alpha\,\psi(s)),$$

where $\alpha$ is a positive constant. In this paper, we refer to this form as Sato profile.

Figure (2) shows the dependence of the normalized potential at the sheath edge, $\Psi_1$, and that at the wall, $\Psi_w$, on the mirror ratio $R_1$ at the sheath edge. For comparison, the corresponding values computed by Sato *et al.* are also shown. It can be seen that our results are in good agreement with Sato *et al.* results especially at low mirror ratios.

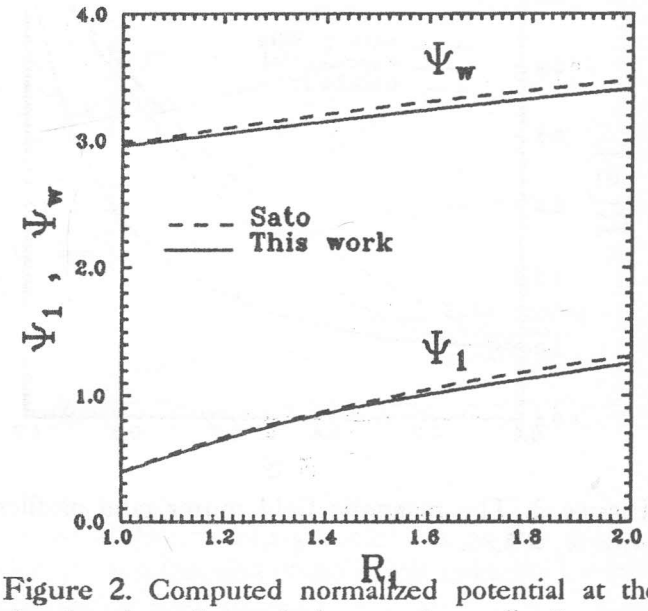


Figure 2. Computed normalized potential at the sheath edge, $\Psi_1$, and that at the wall, $\Psi_w$, as a function of the mirror ratio at the sheath edge, $R_1$, compared to Sato *et al.* results.

To illustrate the effect of the magnetic field mirror ratio profile, we consider, in addition to Sato profile, two other forms which are

1. exponential form given by

$$R(s) = \exp(\alpha s),\ \alpha=1.3558 \text{ and}$$

2. parabolic form, namely,

$$R(s) = -(1-\alpha)s^2+1.,\ \alpha=3.88$$

These three forms of the magnetic field mirror ratio profile are plotted in Figure (3). The mirror ratio $R_1$ at the sheath edge is the same for the three profiles and is set equal to 3.88. The dependence of the normalized electrostatic potential profile on the magnetic mirror ratio profile is illustrated in Figure (4), while the dependence of the normalized plasma density on it is illustrated in Figure (5). As shown, different magnetic mirror ratio profiles even with the same mirror ratio at the sheath edge lead to different profiles for both the potential and the density.

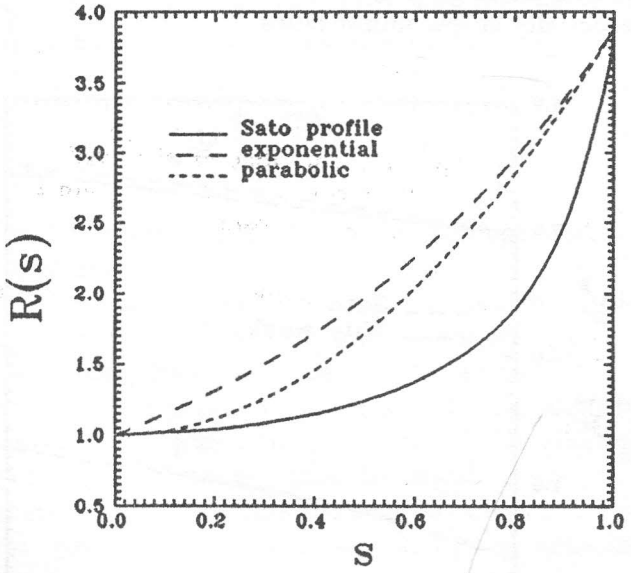


Figure 3. The magnetic field mirror ratio profiles with $R_1$ = 3.88.

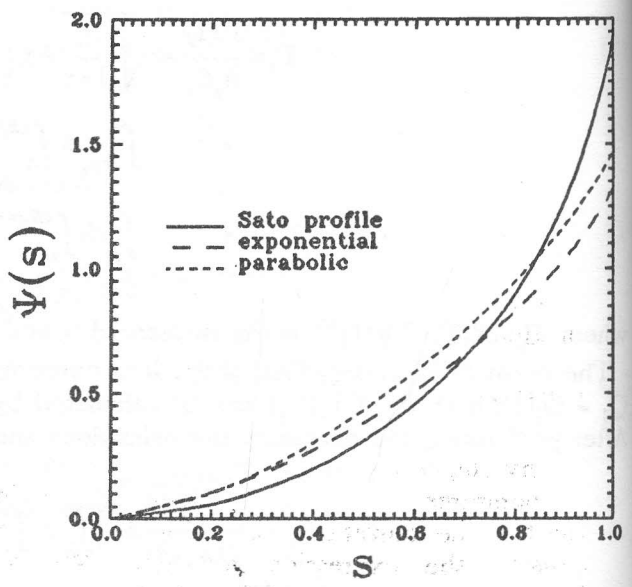


Figure 4. Normalized electrostatic potential profiles in the pre-sheath for the three mirror ratio profiles of Figure (3).

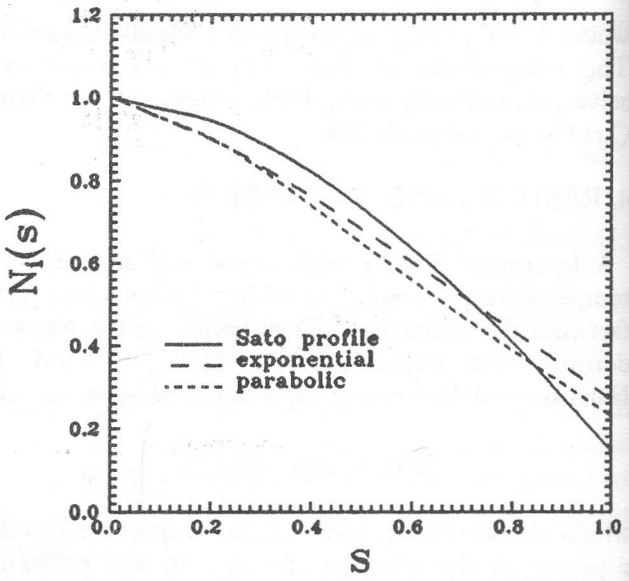


Figure 5. Normalized plasma density profiles for the three mirror ratio profiles of Figure (3).

In Figure (6), the normalized potential at the sheath edge, $\Psi_1$, and that at the wall, $\Psi_w$, are plotted versus the mirror ratio $R_1$ at the sheath edge for the three magnetic mirror profiles. As seen in the Figure, both $\Psi_1$ and $\Psi_w$ increase with $R_1$ for the three profiles. This can be explained by the fact that

as $R_1$ increases, the influence of the acceleration term due to the magnetic field gradient becomes more obvious. The faster motion of the ions results in shorter transit times and hence lower ion density. For quasi-neutrality to be maintained, the normalized electrostatic potential should increase accordingly. It can also be seen from the Figure that the potential drop in the sheath, $\Delta\Psi_s = \Psi_w - \Psi_1$, decreases slightly with the mirror ratio for the three profiles. The variations of the normalized ion mean velocity, $U_1 = \langle v_{//} \rangle_1 / C_s$, the normalized ion particle flux, $\Gamma_1$ and the normalized ion energy flux, $Q_1$, at the sheath edge with $R_1$ are shown in Figures (7), (8) and (9) respectively.

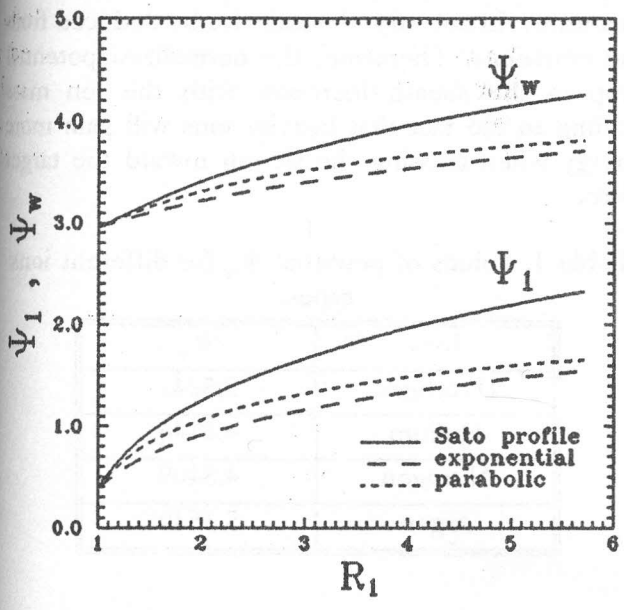


Figure 6. Normalized potential at the sheath edge, $\Psi_1$, and that at the wall, $\Psi_w$, as a function of the mirror ratio at the sheath edge, $R_1$, for the three mirror ratio profiles.

Figure (10) shows the normalized potential profile in the presence of a monotonically falling exponential mirror ratio profile with $R_1$=3.88 for three different particle source spatial distributions namely,

1. $h(s) = \exp(-\nu\,\psi(s))$, with $\nu$=1,
2. uniformly distributed source in the range $0 \le s \le 0.5$,
3. uniformly distributed source in the whole range.

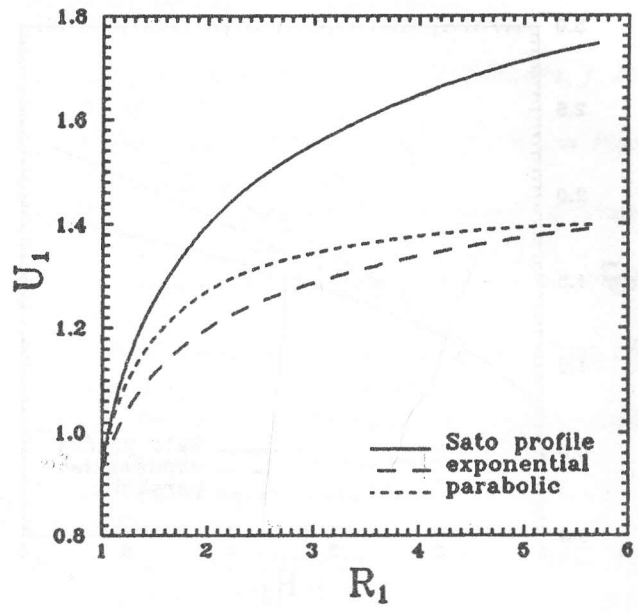


Figure 7. Normalized ion mean velocity at the sheath edge, $U_1$, as a function of the mirror ratio, $R_1$, for the three mirror ratio profiles.

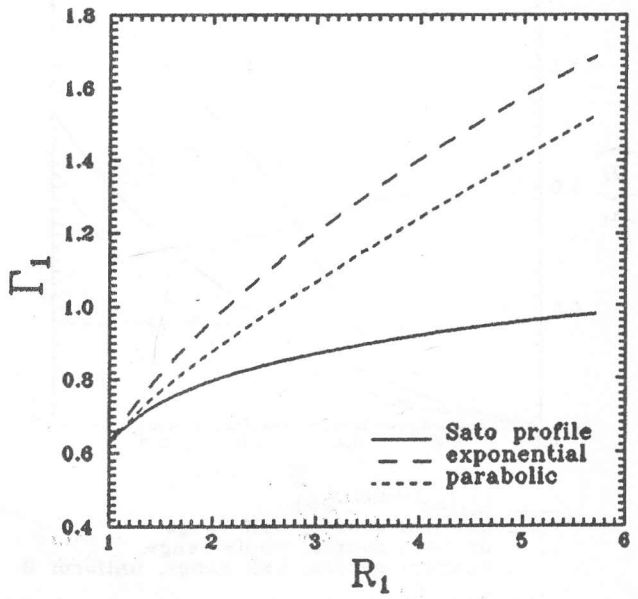


Figure 8. Normalized particle flux at the sheath edge, $\Gamma_1$, as a function of the mirror ratio, $R_1$, for the three mirror ratio profiles.

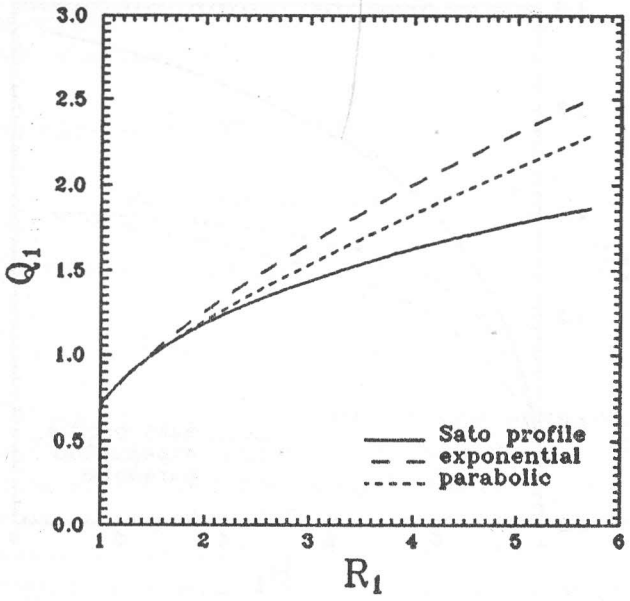


Figure 9. Normalized ion energy flux at the sheath edge, $Q_1$, as a function of the mirror ratio, $R_1$, for the three mirror ratio profiles.

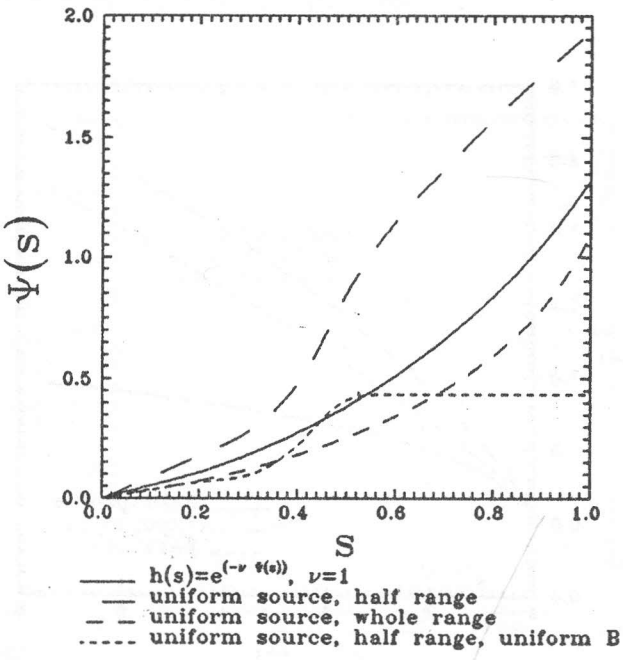


Figure 10. Normalized electrostatic potential profiles in the pre-sheath for three different particle source spatial distributions.

As can be seen, when the magnetic field is not uniform , the potential profile as well as the potentials $\Psi_1$ and $\Psi_w$ are functions of the spatial distribution of the particle source and not just on the integral of the source distribution. Also the potential profile for the case of a uniform source of width 0.5 in a uniform magnetic field is shown. In this case, the potential changes only over the source region and is constant elsewhere. Note that when the nonuniform magnetic field is applied, the potential continues to vary in the sourceless region. This is mainly due to the expansion of the magnetic flux tube.

in addition to the hydrogen plasma, singly ionized helium, nitrogen and argon plasmas, all with $\tau=1$, are considered in an exponential magnetic field profile with $R_1=3.88$. h(s) is kept equal to $e^{-\nu\,\psi(s)}$ with $\nu=1$. Table (1) shows that $\Psi_w$ increases as the ion mass increases. However, all the other normalized quantities do not vary, this can also be deduced from the equations. Therefore, the normalized potential drop in the sheath increases with the ion mass leading to the fact that heavier ions will gain more energy when crossing the sheath toward the target plate.

Table 1. Values of potential $\Psi_w$ for different ions types.

| Ions | $\Psi_w$ |
|---|---|
| Hydrogen | 3.5247 |
| Helium | 4.2146 |
| Nitrogen | 4.8409 |
| Argon | 5.3649 |

## 5. CONCLUSIONS

The plasma-sheath equation for the flow of collisionless plasma to a solid boundary in the presence of an expanding magnetic field has been formulated. The ion source distribution function with a finite temperature chosen by Emmert *et al.* has been used for the formulation. Integrations involved in the plasma equation and in the evaluation of relevant quantities have been solved numerically for various magnetic field profiles. This allowed the solution of the equation for magnetic profiles with mirror ratios higher than those used by Sato *et al.* Results show that the electrostatic

potential formed in the plasma is greatly affected by the applied magnetic field profiles. Increasing the magnetic field mirror ratio at the plasma-sheath edge leads to the increase of the normalized potential at the sheath edge and of the normalized wall potential but to the slight decrease of the normalized potential drop in the sheath. The potential is also affected by the particle source profile. In a nonuniform magnetic field profile, the potential is always varying even in the sourceless region. Consideration of different singly ionized ions leads to the fact that the only normalized quantity that is only influenced is the normalized wall potential which increases as the ion mass increases. This results in the increase of the normalized potential drop in the sheath.

## REFERENCES

[1] S. Saito, M. Sugihara and N. Fujisawa, *j. Nucl. Mater.*, 121, 199, 1984.

[2] J. Derr and J. Shohet, *IEEE Trans. on Plasma Phys.*, PS-9, 234, 1981.

[3] T. Ono, M. Oda, C. Takahashi and S. Matsuo, *J. Vac. Sci. Technol. B*, 4, 696, 1986.

[4] L. Tonks and I. Langmuir, *Phys. Rev.*, 34, 876, 1929.

[5] E.R. Harrison and W.B. Thompson, *Proc. Phys. Soc. London*, 74, 145, 1959.

[6] G. Emmert, R. Wieland, A. Mense and J. Davidson, *Phys. Fluids*, 23, 803, 1980.

[7] R. Bissel and P. Johnson, *Phys. Fluids*, 30, 779, 1987.

[8] K. Sato, F. Miyawaki and W. Fukui, *Phys. Fluids B*, 1, 725, 1989.

[9] W.H. Press *et al.*, *"Numerical Recipes"*, Cambridge University Press, Cambridge, 1989.